VEHICLE DYNAMIC ANALYSIS WITH FLEXIBLE COMPONENTS*

Sang Sup Kim, Ahmed A. Shabana, and Edward J. Haug
Center for Computer Aided Design
College of Engineering
The University of Iowa
Iowa City, Iowa 52242

ABSTRACT. A method is presented for nonlinear, transient dynamic analysis of vehicle systems that are composed of interconnected rigid and flexible bodies. The finite element method is used to characterize deformation of each elastic body and a component mode technique is employed to reduce the number of elastic generalized coordinates. Equations of motion and constraints of the coupled system are formulated in terms of a minimal set of modal and reference generalized coordinates. A Lagrange multiplier technique is used to account for kinematic constraints between bodies and a generalized coordinate partitioning technique is employed to eliminate dependent coordinates. The method is applied to a planar truck model with a flexible chassis and nonlinear suspension components. Simulation results for transient dynamic response as the vehicle traverses a bump, including the effect of bump-stops, and random terrain show that flexibility of the chassis can be routinely accounted for and predicts significant effects on vibratory motion of the vehicle. Compared with a rigid body model, flexibility of the chassis increases peak acceleration of the chassis and induces high frequency vertical acceleration in the range of human resonance, which deteriorates ride quality of off-road vehicles.

1. INTRODUCTION. Modern, lightweight, off-road vehicle systems, operating over rough terrain, have placed increasingly higher demands on the technology required to accurately model and predict dynamic response of a vehicle system. In order to predict dynamic performance of a vehicle, it is necessary to consider nonlinear suspension kinematics and forces, coupled with elastic deformation of the vehicle chassis. Accurate description of vehicle dynamics; e.g., ride comfort and precision of armament subsystems, requires a high resolution mathematical model that accounts for flexibility effects and their coupling with geometrical and suspension force nonlinearities. This is mainly due to the large number of degrees-of-freedom required to model vehicle components and the high degree of geometrical nonlinearity associated with gross motion of suspension components and force-displacement nonlinearity associated with suspension bump-stops. When flexibility is considered, the problem becomes even more difficult, because of the increasing dimensionality and high frequencies of natural vibration.

Some investigators [1-2] have considered flexibility of vehicle components. Their method of analysis is based on a linear theory that has been employed to analyze mechanisms with flexible members [3-5]. In this

*Research Supported by Project No. DAAG29-82-K-0086 U.S. Army Research Office.

analysis, elastic deformation is assumed to have no significant effect on gross motion. Gross motion is first determined, using rigid body analysis and the resulting inertia and reaction forces are introduced in elastic analysis of the components. The total motion of the elastic member is then obtained by superposition of small deformation on gross body motion. There is, however, an increasing demand to produce lighter weight vehicular components that operate at higher speeds. Linear theory assumptions are no longer accurate enough to represent system dynamics, since flexibility effects can significantly affect motion at the driver's station.

Sunada and Dubowsky [6] recently presented a method for the dynamic analysis of flexible mechanisms that couples flexible degrees of freedom with a geometrically nonlinear set of equations of motion. Existing finite element structural programs are combined with a 4×4 matrix dynamic analysis technique. The method has been applied to analyze spatial mechanisms and robotic manipulators. The capability of this method to treat applications such as vehicle systems and space structures without substantial ad-hoc formulation, is not clear. Further, this method neglects rotary inertia of mass that is lumped at individual grid points, in order to avoid the difficulty of using a consistent mass approach to represent inertia coupling between the rigid body motion and the elastic deformation.

Shabana and Wehage [7-8] presented a method for dynamic analysis of large scale inertia-variant flexible systems with coupled reference and elastic deformation. Each flexible body is represented by two sets of generalized coordinates. The first set defines the location and orientation of a body-fixed coordinate system that is rigidly attached to a point on the flexible body. Second, elastic generalized coordinates characterize small deformation relative to the body-fixed system. This set of coordinates is introduced using the finite element method of structural analysis. Modal analysis is employed to reduce the number of elastic degrees of freedom, hence reducing problem dimensionality to manageable extent.

The purpose of this paper is to adapt the automated analysis method of Refs 7-8 for coupled dynamic analysis of planar vehicle systems that are composed of rigid and flexible bodies. As a numerical example, a cross country truck is considered in which the chassis is flexible. This investigation is mainly concerned with analysis of the effect of chassis flexibility on dynamic response of the vehicle, over a single bump and random terrain. A rather simplified tire model is used in this study. Extension of the formulation presented and illustrated here to include a more realistic tire model and three dimensional structural vibration [9] is theoretically simple but involves more detailed calculations than are presented here.

To achieve the above goals, the DADS computer program is used to automatically generate equations of motion, using a Lagrangian formulation. The system equations of motion are solved numerically using a direct integration method and advantage is taken of sparsity of the matrices arising in the formulation. As is shown, this automated formulation is general and conserves manpower that would be required in ad-hoc model formulation and analysis.

2. VEHICLE AND ROAD SURFACE MODELS.

2.1 Vehicle Model. The vehicle used in this investigation is a 5 ton, cross country truck [10] with rigid axles and a Watt mechanism independent suspension. Figure 1 shows the general configuration of the truck. Figure 2 illustrates the wheel suspension, with two suspension support arms beneath the axle and two arms above. Vertical forces are supported by coil springs of progressive stiffness. Figure 3 is an overall view of the frame, which consists of two sidemembers (closed box griders) and several tubular crossmembers that are mounted in holes in the sidemembers and welded to their inner and outer sides. Vehicle parameters used in this analysis are given in Table 1.

Table 1 Vehicle Parameters

Parameter	Value
Gross Vehicle Mass (including payload)	14,400 kg
Vehicle Sprung Mass	11,950 kg
Vehicle Unsprung Mass	2,450 kg
Front axle	1185.0 kg
Rear axle	1185.0 kg
Long trailing arms	44.8 kg
Short trailing arms	35.2 kg
Pitch moment of inertia of sprung mass (about C.M.)	58300.0 kg-m^2
Front and Rear Suspension	
Spring rate (per spring)	6.91×10^5 N/m
Damping rate (per shock absorber)	
Compression	5480.0 N.sec/m
Rebound	17575.0 N.sec/m
Wheel Travel (unloaded)	
Jounce	0.15 m
Tire Quadratic Spring Constant (per tire)	5.649×10^7 N/m^2
Damping rate (per tire)	4625.0 N.sec/m
Tire Radius	0.6 m
Vertical Natural Frequency of Sprung Mass	1.98 Hz
Sprung Pitch Natural Frequency	1.95 Hz

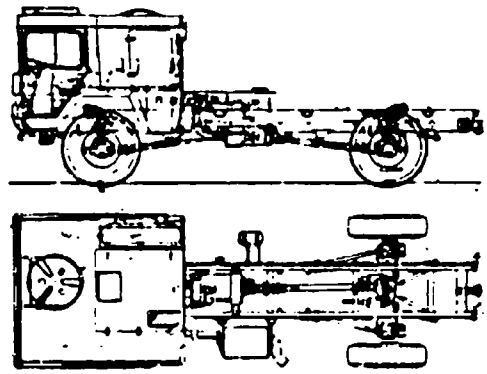

Fig. 1 5 Ton 4x4 Cross Country Truck

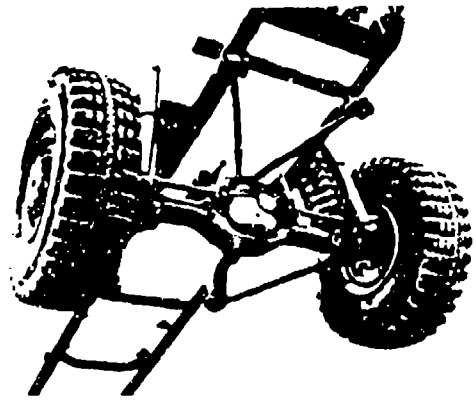

Fig. 2 Wheel Suspension

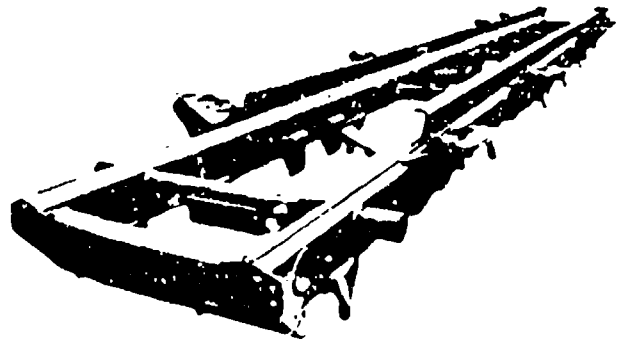

Fig. 3 Main Frame

A simplified, planar rigid body truck model is shown in Fig. 4. Bodies 1 and 2 are the front and rear axle-wheel assemblies, respectively. Each axle-wheel mass is assumed to be concentrated at the wheel center. Body 3 is the chassis of the truck. The mass of the chassis includes masses of the payload and engine. Body-fixed coordinate axes are located at the centroid of each body. Bodies 4, 5, 6 and 7 are the trailing arms that connect the chassis and wheel assemblies by revolute joints. The function of these trailing arms is to provide kinematic control of the axle position and to absorb driving and braking torques acting on the wheels. Therefore, they are modeled as a Watt's mechanism, which gives very small rotation to the axle during vertical displacement. Rigid body data and the initial location and orientation of the body-fixed coordinate systems of each body, with respect to the inertial reference frame, are given in Table 2.

The suspension springs and dampers and the tires are modeled by springs and dampers, as shown in Fig. 5. Spring characteristics of the tires are taken here as quadratic functions of displacement. A simple point contact tire model is used to simulate tire forces that occur due to motion of the wheel relative to the road surface. Fore-and-aft force components are neglected, assuming the tire force is always vertical. The tire is free to leave the ground, to simulate wheel hop. Nonlinear spring and damping characteristics of suspension elements are given in Fig. 6. The high stiffness of the suspension spring in compression, when the spring deflection is greater than 0.15 m, simulates the bump-stop in the suspension system.

A rigid body vehicle model of this vehicle, with five degrees-of-freedom (5-DOF), is also formulated to allow evaluation of the effects of chassis flexibility.

Table 2 Rigid Body Data and Initial Positions

Body No.	Mass (kg)	Moment of Inertia about C.G. ($Kg-m^2$)	Initial Body Coordinates X(m)	y(m)	ϕ(rad)
1	1185	13.33	1.500	0.575	0.0
2	1185	13.33	5.850	0.575	0.0
3	11950	58300	3.675	0.975	0.0
4	22.4	2.38	2.116	0.725	0.464
5	22.4	2.38	5.234	0.725	-0.464
6	17.6	1.14	1.066	0.909	-0.154
7	17.6	1.14	6.284	0.909	0.154

2.2 Road Surface Models. The dynamic response of a vehicle depends strongly on the vertical displacement history of the wheels on the road surface. In this investigation, two roadway models are used, as shown in Fig. 7. Figure 7(a) represents a simulated obstacle with 0.2m height and 0.4m

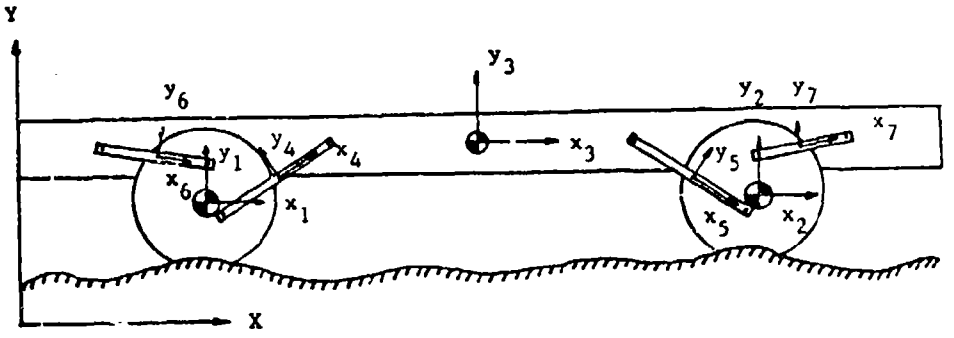

Fig. 4 Rigid Body Truck Model

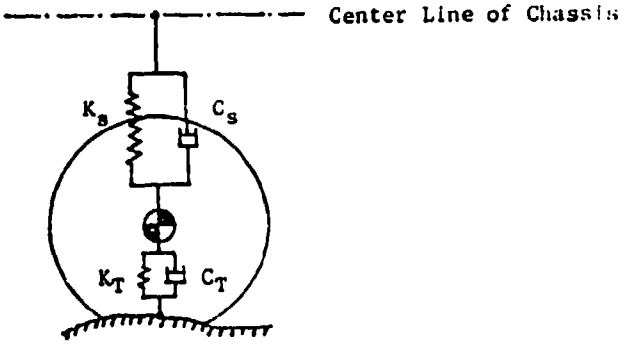

Fig. 5 Suspension and Tire Model

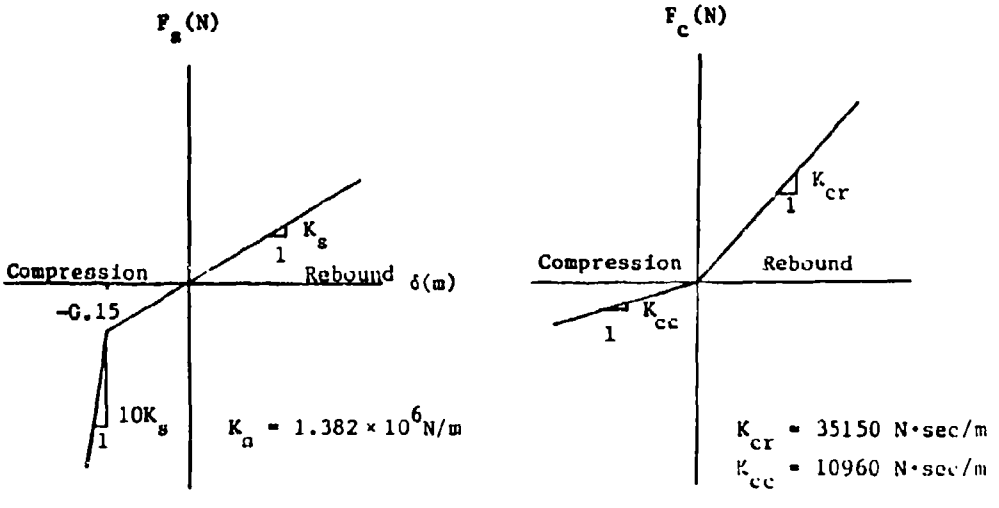

(a) Spring Characteristics (b) Damping Characteristics

Fig. 6 Suspension Characteristics

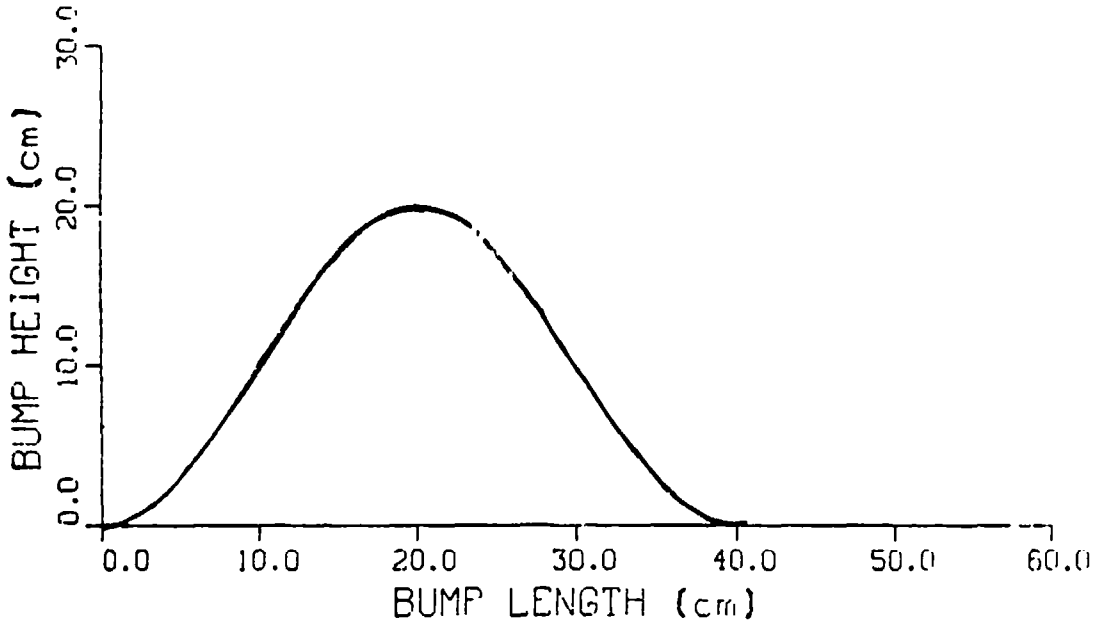

Fig. 7(a) Single Bump Road Profile

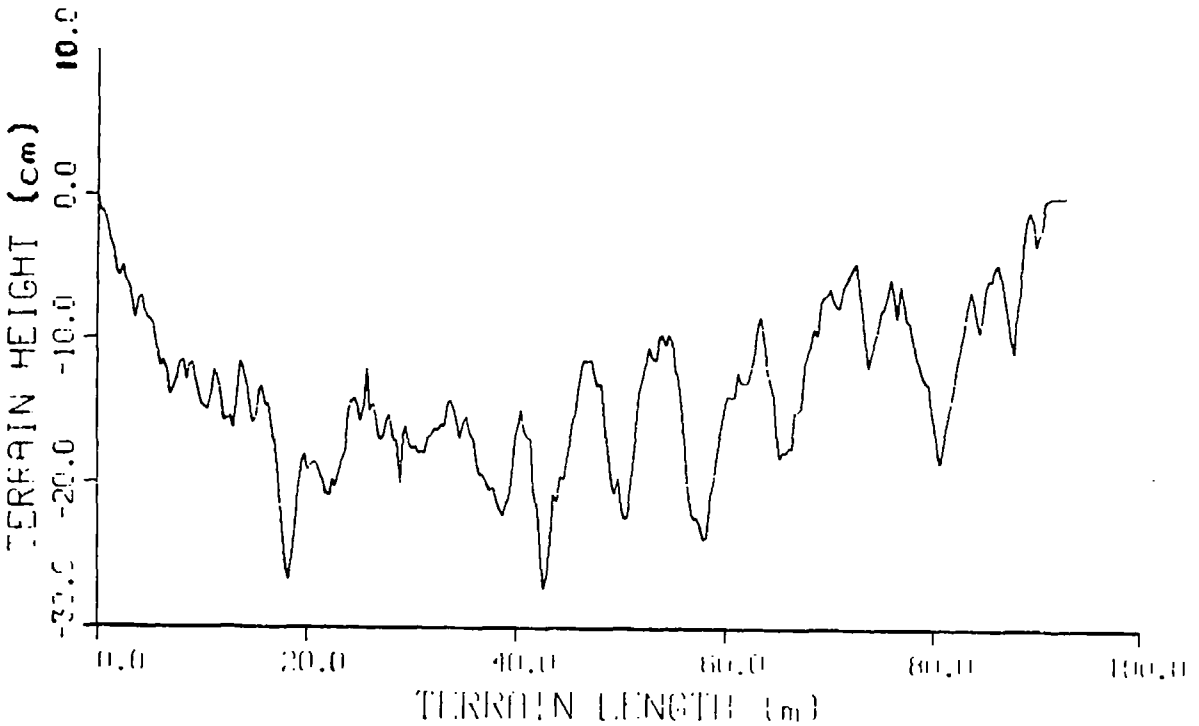

Fig. 7(b) Random Terrain Profile

width, which is used to simulate shock response of the vehicle over a single bump. Figure 7(b) is a terrain profile with a RMS roughness of 2.64cm (1.04 in) and a length of 91.44m (300 ft).

3. ANALYTICAL APPROACH. The analysis method employed in this investigation is similar to the method used in Refs. 7-8 to analyze mechanical systems with interconnected rigid and flexible bodies. In this method, the chassis of the vehicle is considered as a deformable substructure. Two sets of generalized coordinates are employed to describe the flexible body configuration. First, reference generalized coordinates define the location and orientation of a body-fixed coordinate system on each body. Second, a set of elastic coordinates define small deformation of each body, relative to its body-fixed coordinate system. This set is introduced using the finite element method.

Kinetic and strain energy expressions are developed for the individual elements. The kinetic and strain energy of each body are obtained by summing energies of its elements. Constraints between different elements of a body are expressed in a Boolean form and constraints between different bodies are introduced using a Lagrange multiplier technique. The generalized coordinate partitioning method [11] and a component mode structural analysis technique are employed to describe the system equations of motion, with a minimal set of independent generalized coordinates [7,8]. The method of Refs. 7 and 8 is summarized here, for completeness.

3.1 Energy Expressions. Figure 8 shows a typical element j of a two dimensional planar flexible body i. Let the x-y coordinate system represent an inertial reference frame and the x^i-y^i system represent a coordinate system that is rigidly attached to body i.

The location of an arbitrary infinitesimal volume at point p^{ij} on element j can be defined as

$$\underline{R}_p^{ij} = \underline{R}^i + A^i \underline{r}^{ij} \tag{1}$$

where $\underline{R}^i = [x^i, y^i]^T$ is the vector of translational coordinates of the origin of the coordinate system of body i with respect to the x-y system,

$$A^i = \begin{bmatrix} \cos\theta_i & -\sin\theta_i \\ \sin\theta_i & \cos\theta_i \end{bmatrix} \tag{2}$$

is the transformation matrix from x^i-y^i to x-y coordinate systems, and $\underline{r}^{ij}$ is the position vector of p^{ij} with respect to the x^i-y^i system, defined as

$$\underline{r}^{ij} = \underline{r}_0^{ij} + \underline{W}^{ij} \tag{3}$$

where $\underline{r}_0^{ij}$ is the position vector of p^{ij} in the undeformed state and $\underline{w}^{ij}$ is the elastic displacement vector in the body fixed coordinate system. Let an x^{ij}-y^{ij} coordinate system be attached to the left end of element j. Using a shape function, $\underline{r}^{ij}$ can be expressed in terms of nodal coordinates $\underline{e}_k^{ij}$ (k = 1,2...6), which represent nodal coordinates and slopes of reference lines at nodes, relative to the x^i-y^i system,

$$\underline{r}^{ij} = N^{ij}\underline{e}^{ij} \tag{4}$$

where N^{ij} is the element shape function.

From Eq. 1, the position vector $\underline{R}_p^{ij}$ can be expressed [7-8], in terms of reference coordinates (x^i, y^i, θ^i) and nodal coordinates $(\underline{e}^{ij})$, as

$$\underline{R}_p^{ij} = \underline{R}^i + A^i N^{ij}\underline{e}^{ij} \tag{5}$$

Differentiating Eq. 5 with respect to time gives

$$\dot{\underline{R}}_p^{ij} = \dot{\underline{R}}^i + \dot{A}^i N^{ij}\underline{e}^{ij} + A^i N^{ij}\dot{\underline{e}}^{ij} \tag{6}$$

where

$$\begin{aligned}\dot{A}^i &= \dot{\theta}^i \begin{bmatrix} -\sin\theta^i & -\cos\theta^i \\ \cos\theta^i & -\sin\theta^i \end{bmatrix} \\ &= \dot{\theta}^i A^{i'}\end{aligned} \tag{7}$$

Substituting Eq. 7 into Eq. 6 and writing the result in partitioned form yields

$$\dot{\underline{R}}_p^{ij} = \begin{bmatrix} I & A^{i'}N^{ij}\underline{e}^{ij} & A^i N^{ij} \end{bmatrix} \begin{Bmatrix} \dot{\underline{R}}^i \\ \dot{\theta}^i \\ \dot{\underline{e}}^{ij} \end{Bmatrix} \tag{8}$$

The kinetic energy expression for element ij is given by

$$\begin{aligned}T^{ij} &= \frac{1}{2}\int_{V^{ij}} \rho^{ij}\, \dot{\underline{R}}_p^{ij\,T}\, \dot{\underline{R}}_p^{ij}\, dV^{ij} \\ &= \frac{1}{2}\dot{\underline{q}}^{ij\,T} M^{ij}\, \dot{\underline{q}}^{ij}\end{aligned} \tag{9}$$

where V^{ij} is the element volume, ρ^{ij} is density of the element material,

$$\underline{q}^{ij} = [\ \underline{R}^{i^T}\ \theta^i\ \underline{e}^{ij^T}\ ]^T \tag{10}$$

are the generalized coordinates of element ij and M^{ij} is the element mass matrix [7-8]. The vector e^{ij} can be written as

$$\underline{e}^{ij} = \underline{e}_0^{ij} + \underline{q}_f^{ij} \tag{11}$$

where $\underline{e}_0^{ij}$ is the vector of nodal coordinates in the undeformed state and $\underline{q}_f^{ij}$ is the vector of deformations at the nodes, defined with respect to the body-fixed coordinate system.

The total kinetic energy of body i is given by

$$T^i = \sum_{j=1}^{n^i} T^{ij}$$

$$= \frac{1}{2}\,\dot{\underline{q}}^{i^T} M^i\, \dot{\underline{q}}^i \tag{12}$$

where $\underline{q}^i = [\ \underline{R}^{i^T}\ \theta^i\ \ \underline{q}_f^{i^T}\ ] = [\ \underline{q}_r^{i^T}\ \ \underline{q}_f^{i^T}\ ]$, $\underline{q}_r^i$, and $\underline{q}_f^i$ represent, respectively, reference and elastic coordinates of body i. The strain energy of body i can also be expressed in compact form as [7-8]

$$U^i = \frac{1}{2}\,\underline{q}^{i^T} K^i\, \underline{q}^i \tag{13}$$

where K^i is the stiffness matrix of body i.

The virtual work of external forces acting on body i can be written as

$$\delta W^i = \underline{Q}^{i^T}\, \delta \underline{q}_i \tag{14}$$

where $\underline{Q}^i$ is the vector of generalized forces associated with the generalized coordinates of body i.

3.2 Equations of Constraint. When adjacent bodies are connected, nonlinear constraint equations are written between adjacent bodies and a Lagrange multiplier method is employed to adjoin these constraint equations to the equations of motion. These constraints permit the joining of elastic bodies, rigid bodies, or rigid and elastic bodies. Points of attachment on elastic bodies are at nodes of the finite element model. In general, equations of constraint can be written, in vector function form, as

$$\underline{\Phi}(\underline{q},t) = 0 \tag{15}$$

where $\Phi(q,t) = [\ \phi_1(q,t),\ldots,\phi_m(q,t)]^T$. This is a set of nonlinear algebraic equations, which can be used to describe constraints between vehicle components.

3.3 Equations of Motion. The composite vector of all system generalized coordinates is designated as $\underline{q} = [\underline{q}^{1T}, \underline{q}^{2T}, \ldots \underline{q}^{NT}]^T$, where N is the total number of bodies (substructures) in the system. The constraint equations of Eq. 15 are assumed to be independent. Presuming that the constraints are workless, the variational form of the equations of motion [12] for body i, where subscript notation denotes differentiation with respect to a vector, is

$$\frac{d}{dt}\ T^i_{\underline{\cdot}\underline{q}^i} - T^i_{\underline{q}^i} + U^i_{\underline{q}^i} - \underline{Q}^{iT}\ \delta\underline{q}^i = 0 \tag{16}$$

for all virtual displacements $\delta\underline{q}^i$ that are consistent with constraints of Eq. 15. It can be shown that introducing the vector $\underline{\lambda}^T\ \underline{\Phi}_{\underline{q}i}$ into Eq. 16 allows the coefficients of $\delta\underline{q}^i$ to be set to zero [13]. Thus,

$$\frac{d}{dt}\ T^i_{\underline{\cdot}\underline{q}^i}{}^T - T^i_{\underline{q}^i}{}^T + U^i_{\underline{q}^i}{}^T - \underline{Q}^i + \underline{\Phi}^T_{\underline{q}i}\underline{\lambda} = 0 \tag{17}$$

with T^i, U^i, and $\underline{Q}^i$ given by Eqs. 12, 13, and 14.

3.4 Generalized Coordinate Reduction. Efficient solution of the system equations of motion requires a transformation from the space of system nodal generalized coordinates to the space of system modal generalized coordinates, which has lower dimension. The method presented in Refs 7-8 is based on solving the eigenvalue problem for each substructure once. From Fourier analysis of the forcing functions, an initial estimate of the number of modes to be retained is made. During the simulation, additional eigenvectors are recalled or deleted, as required. For the purpose of determining eigenvalues and eigenvectors, if a substructure is assumed to vibrate freely about a reference configuration, Eq. 17 yields

$$\bar{M}^i_{ff}\ \ddot{\underline{P}}^i_f + \bar{K}^i_{ff}\ \underline{P}^i_f = 0 \tag{18}$$

Where $\bar{M}^i_{ff}$ and $\bar{K}^i_{ff}$ are the mass and stiffness matrices associated with the nodal generalized coordinates and $\underline{P}^i_f$ is the vector of elastic coordinates after imposing the body-fixed coordinate conditions. The stiffness matrix $\bar{K}^i_{ff}$ is positive definite, because the reference coordinate system is fixed. Equation 18 yields a set of eigenvectors and a modal matrix. A

coordinate transformation from the physical nodal coordinates to modal coordinates is defined by

$$\underline{P}_f^i = B_2^i \underline{X}^i \tag{19}$$

where B_2^i is the modal matrix, consisting of the eigenvectors obtained from Eq. 18 and $\underline{X}^i$ is a vector containing the modal coordinates. Using Eq. 19, the reference and nodal generalized coordinates are written in terms of reference and modal coordinates. A substantial reduction in problem dimensionality can be achieved by considering only significant modes.

4. NUMERICAL RESULTS. In order to take the effect of flexibility of vehicle components on global vehicle motion into account, the chassis (Body 3) and long trailing arm (Body 4) are modeled as elastic bodies. The chassis and long trailing arm are divided into 12 and 2 finite beam elements, respectively, with reference coordinates located at their midpoints. The flexural rigidity of each flexible member is calculated using the cross-sectional area of the beam and its material properties. Lateral and axial deformation are considered.

The flexible components are initially treated as substructures that are fixed at their midpoints. Since each beam element has 6 degrees-of-freedom, the flexible chassis has a total of 36 elastic degrees-of-freedom and each flexible link has 6 elastic degrees-of-freedom. The eigenvalue problem is solved for each of these substructures. The lowest six natural frequencies of the flexible chassis are 6.11, 6.11, 38.31, 38.31, 83.36, and 83.36 Hz, where the first four modes are bending modes and the fifth and sixth modes are axial vibration modes. The lowest two natural frequencies of the flexible links are 88.92 and 88.92 Hz. One percent structural damping is considered for every chassis mode of vibration.

4.1 Vehicle Response over Single Bump. The vehicle travels over the single bump given in Fig. 7(a), with a vehicle speed of 3 m/sec (6.7 miles/hr). The simulation is carried out for two vehicle models, rigid and flexible chassis, to evaluate flexibility effects of the chassis on vehicle motion. To compare higher mode effects of the flexible chassis model, 2- and 4-mode solutions are obtained. Figure 9 shows the vertical displacement of the center of mass of the chassis, from its static equilibrium position. The figure shows significant peak differences between vertical displacement of rigid and flexible chassis models. Figure 9 also shows that the contribution of higher vibration modes to vertical displacement of the chassis is negligible.

The vertical acceleration at the center of mass of the chassis is given in Fig. 10, for each model. It shows that chassis flexibility results in increased peak acceleration and significantly higher frequency content during passage over the bump. The effect of structural damping on the vehicle response is shown in Fig. 11. In this figure the vertical acceleration of the chassis with and without damping are plotted. The damped response decays with time, while the undamped response has a sustained oscillation.

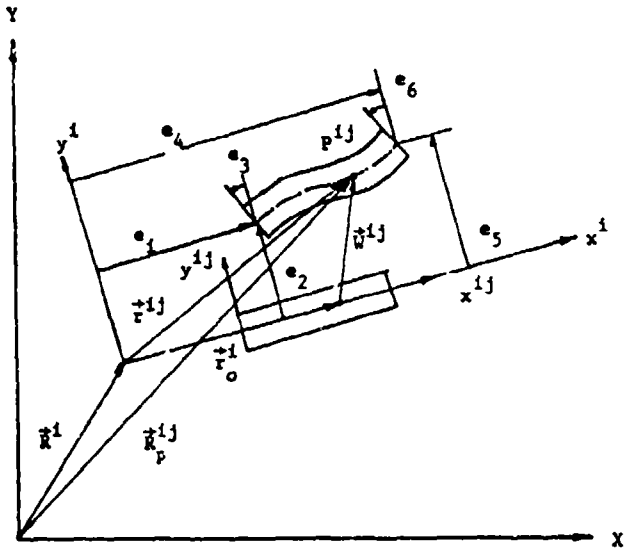

Fig. 8 Generalized Coordinates of a Beam Element

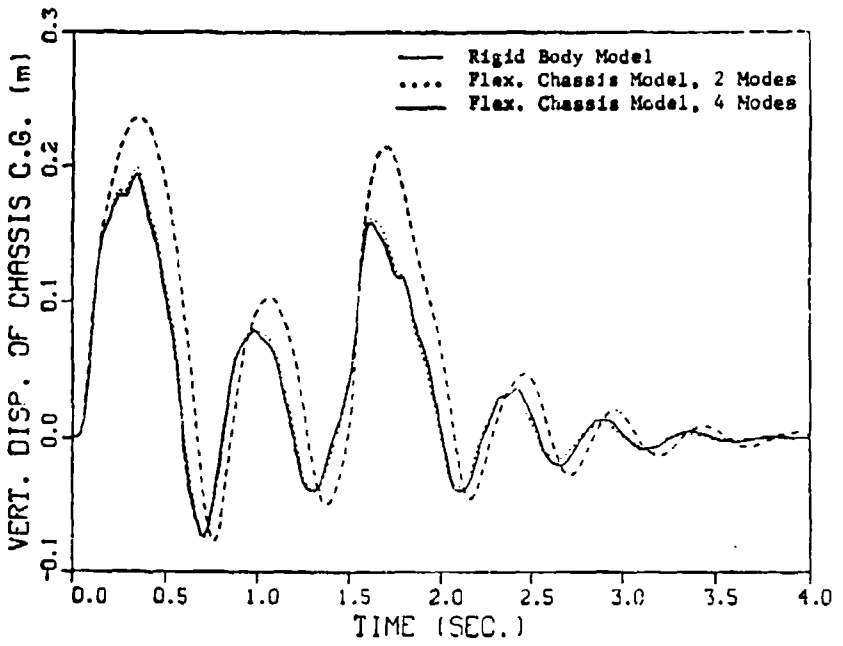

Fig. 9 Vertical Displacement of the Chassis C.G. over Single Bump

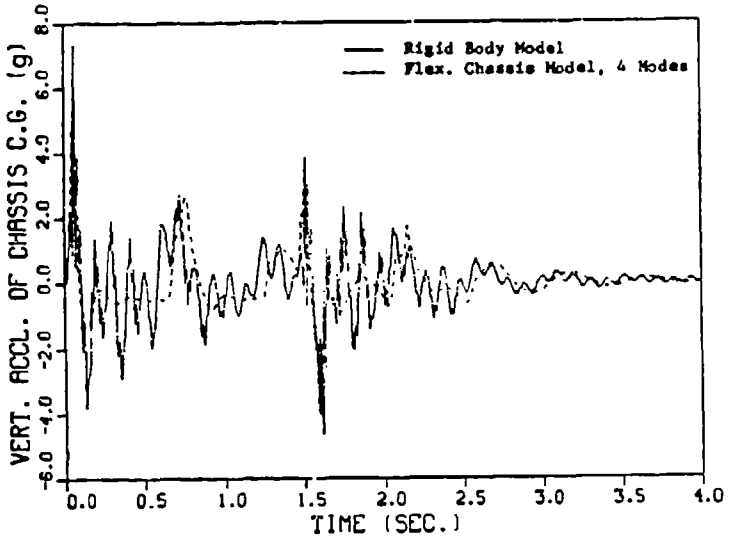

Fig. 10 Vertical Acceleration of the Chassis C.G. over Single Bump

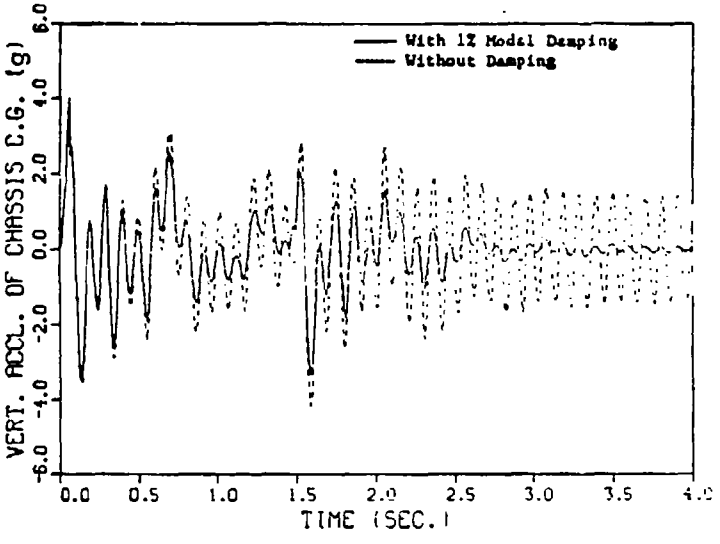

Fig. 11 Effect of Structural Damping on Vertical Acceleration of Chassis C.G. over Single Bump, Flex, Chassis Model, 2 Modes

Computation time for the rigid model simulation was 7.0 minutes on a PRIME 750 supermini computer. Computation times with the two and four mode flexible chassis models were 2.08 and 5.18 times the computation time of the rigid model. This shows that computational efficency can be obtained by using the smallest number of modes required to obtain reasonable accuracy.

4.2 Vehicle Response over Random Terrain. Simulation is carried out over the terrain given in Fig. 7(b) for the rigid model, the two and four mode flexible chassis models, the two mode flexible links model, and the two mode flexible chassis and links model. Vehicle velocity is 7.5 m/sec. (16.8 miles/h). Results are given in Figs. 12 to 14. Since link flexibility does not have significant effect on the global vehicle motion, results for the model with flexible links are not included.

Figure 12 shows vertical displacement at the center of mass of the chassis. No significant difference is observed between rigid and flexible models. No significant difference has been found between the two and four-mode solution of the flexible chassis models. It has also been found that there is no significant difference in vertical chassis displacement between the two mode flexible chassis and links model and the two mode flexible chassis model. It is concluded that flexibility effects of the stiff link (which has relatively high natural frequency) on the vehicle response may be neglected.

Figure 13 shows vertical acceleration at the center of mass of the chassis. Flexibility of the chassis results in a significant increase in the acceleration level at the center of the chassis and high frequency content near the resonant frequency of the human body. Vibration in the chassis may thus result in an unpleasant motion and deteriorate ride comfort of the vehicle. Suspension link flexibility does not have noticeable effects on the vertical acceleration of chassis.

Deflection of the front end of the chassis, with respect to its body-fixed coordinate system, is given in Fig. 14. Dynamic peak deflections for the two mode flexible chassis model is 22 times the static deflection of that model. The frequency of vibration of the front of the chassis is about 6 Hz, which is the fundamental natural frequency of the chassis.

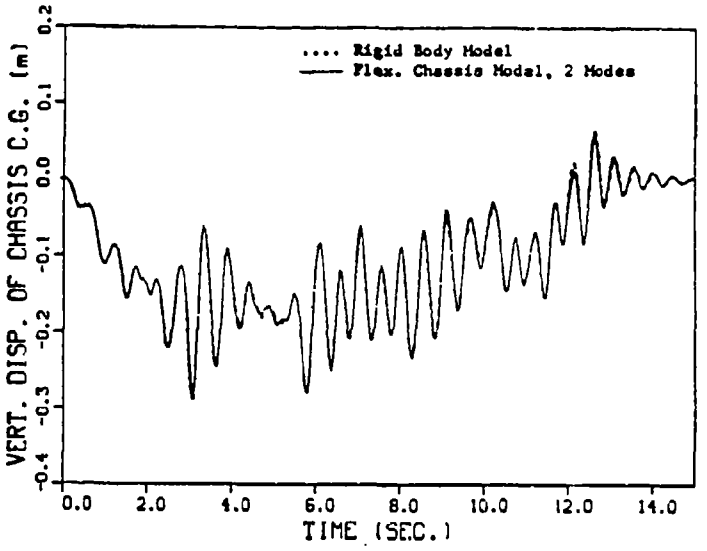

Fig. 12 Vertical Displacement of Chassis C.G. over Random Terrain

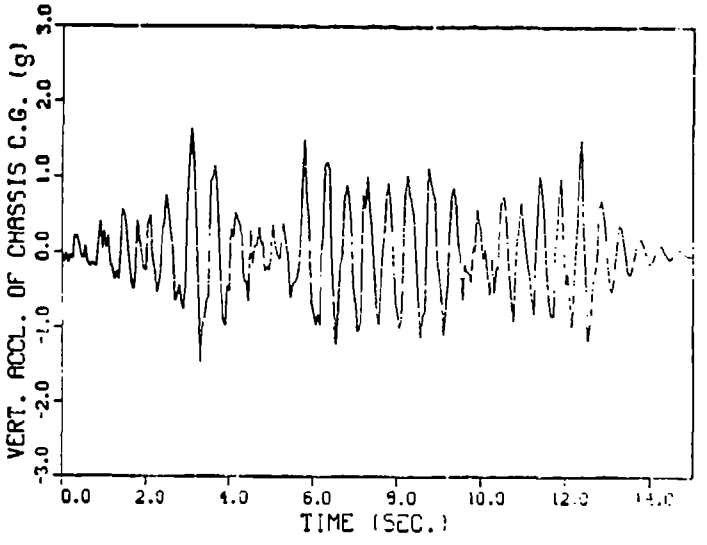

(a) Rigid Body Model

Fig. 13 Vertical Acceleration of Chassis C.G. over Random Terrain, 2 Modes

(Fig. 13 continued)

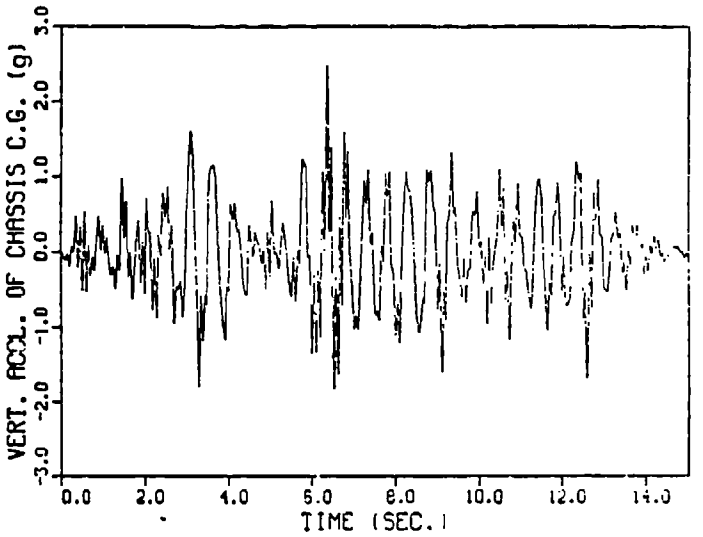

(b) Flex. Chassis Model

Fig. 13 Vertical Acceleration of Chassis C.G. over Random Terrain, 2 Modes

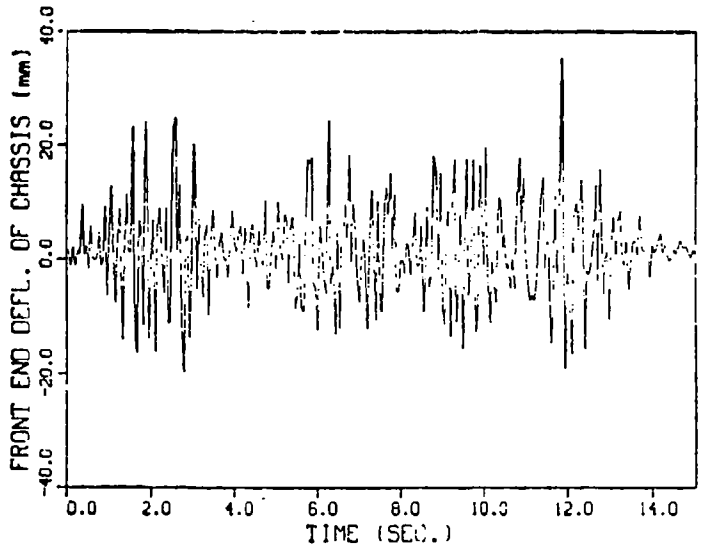

Fig. 14 Front End Deflection of Chassis over Random Terrain, Flex. Chassis Model, 2 Modes

References

1. Vail, C.F., "A Modal Synthesis Technique for Determining Properties for Structures for Mass and Stiffness Changes," SAE paper 740329, 1974.

2. Elmadany, M.M., Dokanish, M.A., and Allan, A.B., "Ride Dynamics of Articulated Vehicles - A Literatures Survey," Vehicle Systems Dynamics, Vol. 8, 1979, pp.289-316.

3. Winfrey, R.C., "Elastic Link Mechanism Dynamics," ASME Journal of Engineering for Industry, Feb. 1971, pp. 268-272.

4. Sadler, J.P., and Sandor, G.N., "A Lumped Parameter Approach to Vibration and Stress Analysis of Elastic Linkages," ASME Journal of Engineering for Industry, May 1973, pp. 549-557.

5. Erdman, A.C., Sandor, G.N., and Oakberg, R.G., "A General Method for Kineto-Elastodynamic Analysis and Synthesis," ASME Journal of Engineering for Industry, Nov. 1972, pp. 1193-1205

6. Sunada, W., and Dubowsky, S., "The Application of Finite Element Methods to the Dynamic Analysis of Flexible Spatial and Co-planar Linkage Systems," ASME Journal of Mechanical Design, July 1981, Vol. 103, pp. 643-651.

7. Shabana, A. and Wehage, R.A., "Variable Degree of Freedom Component Mode Analysis of Inertia-Variant Flexible Mechanical Systems," ASME paper No. 82-DET. 93, Journal of Mechanisms, Transmissior and Automation in Design, to appear.

8. Shabana, A., and Wehage, R.A., "A Coordinate Reduction Technique for Dynamic Analysis of Spatial Substructures with Large Angular Rotations," Journal of Strucutral Mechanics, to appear, Dec. 1983.

9. Shabana, A.A. and Wehage R.A., "Spatial Transient Analysis of Inertia-Variant Flexible Mechanical Systems", Submitted to ASME Journal of Mechanical Design, Jan. 1983.

10. Klanner, R., "Cross-Country Truck for Fast Off-Highway Navigation, 6th International Conference of International Society of Terrain and Vehicle Systems," Vienna, Aug. 1978, pp. 22-25.

11. Wehage, R.A. and Haug, E.J., "Generalized Coordinate Partitioning for Dimension Reduction in Analysis of Constrained Dynamic Systems," ASME Journal of Mechanical Design, Vol. 104, 1982, pp. 247-255.

12. Goldstein, H., Classical Mechanics, Addison Wesley, 1980.

13. Haug, E.J. and Arora, J.S., Applied Optimal Design, Wiley 1979.